TEST OF A SOLAR-HYBRID MICROTURBINE SYSTEM AND EVALUATION OF STORAGE DEPLOYMENT

Lars Amsbeck[1], Thorsten Denk[2], Miriam Ebert[3], Christian Gertig[4], Peter Heller[3], Patrik Herrmann[3], Jens Jedamski[1], Joachim John[5], Robert Pitz-Paal[6], Tobias Prosinečki[7], Jonny Rehn[8], Wolfgang Reinalter[3] and Ralf Uhlig[1]

[1]German Aerospace Center (DLR), Institute of Technical Thermodynamics, Solar Research, Pfaffenwaldring 38-40, 70372 Stuttgart, Germany, +49-711-6862-306, Lars.Amsbeck@dlr.de

[2] CIEMAT, Plataforma Solar de Almeria, Spain

[3]German Aerospace Center (DLR), Institute of Technical Thermodynamics, Solar Research, Plataforma Solar de Almeria, Spain

[4]Abengoa Solar New Technologies, Sevilla, Spain

[5]GEA Technika Cieplna Sp. z o. O, Opole, Poland

[6]German Aerospace Center (DLR), Institute of Technical Thermodynamics, Solar Research, Cologne, Germany

[7]Royal Institute of Technology (KTH), Stockholm, Sweden

[8]Turbec, Malmö, Sweden

Abstract

A solar-hybrid microturbine system using a tube receiver and a Turbec T100 was tested at the Plataforma Solar de Almería. The design receiver outlet temperature of 800°C was achieved with an open receiver aperture and also using a pressureless quartz window. Measured receiver efficiencies of 39.7% for the open receiver at 782°C outlet temperature and 44% at 803°C outlet temperature for the configuration with the window are much lower than the design values due to design flaws in the cavity insulation and a too low mass flow from the turbine. Nevertheless, the encountered problems are solvable and further lessons learned are given.

For a commercial system design using small heliostats of 1m^2-mirror area a peak receiver efficiency of >85% was simulated using a face-down receiver configuration with a much smaller aperture. The solar-hybrid system can also be combined with a pressurized pebble-bed heat storage. For an off-grid application a solar share of 82% was simulated.

Keywords: Solar tower, microturbine, tube receiver, solar-hybrid, heat storage, off-grid

1. Introduction

Diesel generator sets are the major power source in off-grid applications today. In view of roughly 1.6 billion people without electricity worldwide the replacement of Diesel gensets in sunny locations could be a reasonable market for solar-hybrid microturbine systems.

In such a system a commercially available microturbine is connected to a pressurized solar air receiver located on the tower of a small heliostat field. The development of a metallic tube receiver was presented in [1]. A test system was installed at the Plataforma Solar de Almería, Spain. Fig. 1 shows the main components of the system setup: Turbec T 100 microturbine (1), inlet pipe (2), distributor (3), 40 expansion joints (4), 40 absorber tubes with 26.7mm OD and 2.11mm wall thickness, each 2.5m long and equipped with a wire-coil heat transfer enhancement with a wire diameter of 2mm and a pitch of 55mm (5), collector (6) and outlet pipe (7), both with inner insulation, the combustion chamber (8) , the cavity (9) and an optional pressureless quartz window with anti-reflection coating (10). The quartz window consists of 10 strips of 60°-tube segments with the concave side oriented to the heliostats [2]. The strips are installed loosely one beside the other, forming a quasi-flat window.

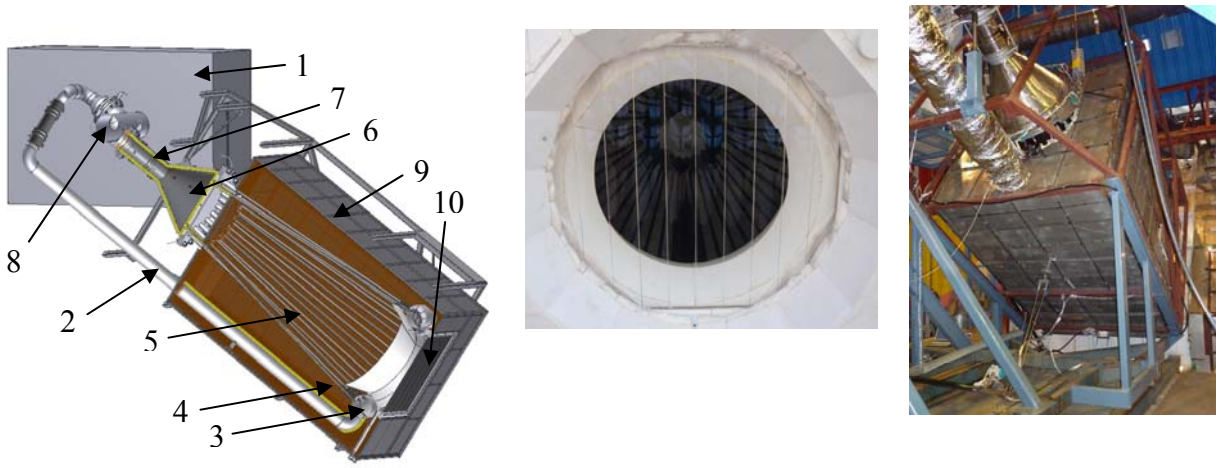

Fig. 1: Cross-section of the solar-hybrid microturbine system (left) and pictures of the receiver aperture with the quartz window(middle) and the cavity (right)

2. Receiver Tests

2.1 General

The receiver was designed for an air inlet temperature of 600°C and a maximum air outlet temperature of 800°C, at a pressure of up to 4.5bar$_a$. Tests with the receiver connected to the microturbine started in February 2010 at the CESA-1 tower of the Plataforma Solar de Almeria and were finished at the end of June 2010. In a first campaign the receiver was tested with an open aperture, followed by a second campaign with the quartz window covering the aperture.

2.2 Measurement system

The system is equipped with thermocouples at the inlet and outlet of the receiver, at the outlet of every absorber tube and on 5 positions on the not directly irradiated side of four absorber tubes. Absolute pressure and pressure drop over the receiver are measured as well as the mass flow with a Pitot tube.

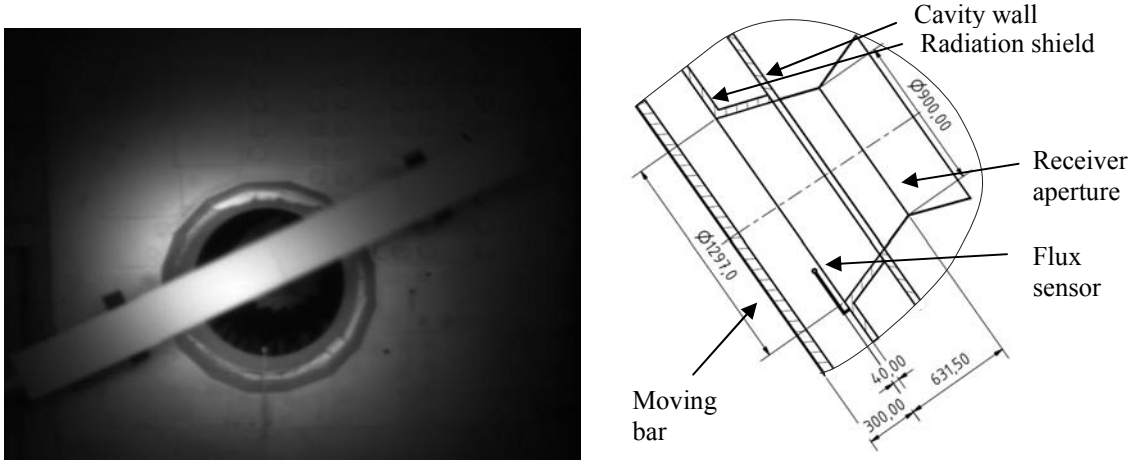

Fig. 2: Flux measurement system (left) and cross section of the receiver aperture area (right)

The incident solar radiation is measured using a system consisting of a camera, a moving bar and a heat flux sensor as shown in Fig**. 2**. The moving bar with its highly diffuse reflecting shields rotates through the aperture region while the camera takes a series of pictures to combine them to a complete flux map. This flux map is calibrated using the flux sensor. As the moving bar, the receiver aperture and the flux sensor are not located in the same plane (see Fig**. 2**) the incoming solar radiation cannot be directly calculated from the measured flux map. Compared to a configuration where the moving bar is directly in front of the aperture and flux sensor additional errors are introduced. Ray-tracing calculations using deflectometry data of all

heliostats to model the reflective surface and the geometry of the radiation shield have been used to determine the solar receiver input power and the error of this evaluation.. A diffuse reflectivity of 95% of the white ceramic radiation shield material is assumed for the ray-tracing calculations, as absorbed power is mainly also diffusely re-radiated and contributes to the input power. The quite high tracking error of the heliostat field further contributed to the errors of the evaluation method.

The receiver input is determined according to the following steps:

1. Determination of the average aim point: In the ray-tracing process all heliostats are set on the same aimpoint and this aimpoint is changed until the calculated flux map in the moving bar plane shows the same center as the measured flux map. It is assumed that the aimpoint is in a plane orthogonal to the north direction in the receiver aperture middle.
2. Tracking error: A statistical tracking error with a Gaussian distribution is imposed on the aimpoints of the heliostats and the standard deviation is changed until the best conformity with the measured distribution is achieved.
3. Moving bar evaluation diameter: The diameter in the moving bar plane from where solar radiation enters the aperture in the radiation shield is determined using ray-tracing runs with the statistical deviation from the second step.
4. Ray-tracing runs: A sufficient number of ray-tracing runs with different sets of statistically distributed aimpoints is performed and the power into the receiver, into the flux sensor, into a projection of the flux sensor onto the moving bar plane and into the diameter on the moving bar plane from step 3 are calculated.
5. Intensity calibration factor: The ratio of the flux sensor flux and the flux at the projection onto the moving bar plane and the standard deviation of the ratio are determined from the calculations in 4.
6. Evaluation of the measured flux map: the measured flux map is calibrated with the intensity calibration factor ratio and the power through the moving bar plane diameter is calculated.
7. Receiver input power: All ray-tracing runs from step 4 are calibrated to have the same power into the moving bar evaluation diameter and then the mean power into the receiver aperture and its standard deviation are calculated.

Mean deviations from the calibration of the moving bar from the flux sensor in a 300mm distant plane are ~2.5% and mean deviations for the solar input power due to the unknown exact aimpoints are also ~2.5% for statistical tracking errors <3mrad. The error of the solar input measurement increases therefore from -4.7%..+4.1% [3] to -5.88%..+5.4%.

2.3 Results

The receiver achieved its design outlet temperature of 800°C with an open aperture, but only for a couple of short times before the temperature limits at the collector plate were exceeded due to unexpected hot air streams through the cavity walls. Quasi-stationary conditions were only achieved up to ~780°C outlet temperature. The problems with the collector plate were solved before the second measurement campaign with the quartz window by using the outlet stream of the turbine-receiver-interface cooling fan to provide additional cooling. In the second campaign the 800°C outlet temperature was achieved on a regular basis and for long durations.

A total of more than 100h of solar operation and of more than 160h of turbine operation were achieved. This also included the first solar-only gas turbine operation worldwide as known to the authors. At 800°C receiver outlet temperature an unplanned closure of the fuel valves reduced the turbine power to ~12kW_{el}, but a stable solar-only operation was achieved.

No failures at the metallic, pressurized parts of the receiver occurred during the tests. Only some downward bending of the absorber tubes of about 1-2cm was observed at the end of the test time which could be a stress relaxation effect.

2.3.1 Operation with open aperture

All measured values were averaged over one minute.

Date and time	19.05.2010 12:50		
DNI	940.5 W/m^2	Avg. absorber tube outlet temperature	790.2°C
Number of heliostats	46	Absolute humidity	1.72 g/kg
Wind speed	3.8 m/s	Receiver pressure in the inlet pipe	3.75 bar$_a$
Wind directions	213.8°north	Mass flow	0.516 kg/s
Turbine power	69.98 kW	Pressure drop	70.4 mbar
Turbine speed	96.4%	Solar input	272.8 kW
Receiver inlet temperature	597.7°C	Thermal receiver power	108.3 kW$_{th}$
Receiver outlet temperature	782.2°C	**Receiver efficiency**	**39.7%**

Table 1: Results of operation with open aperture

2.3.2 Operation with a pressure-less quartz window

All measured values were averaged over one minute.

Date and time	23.06.2010 12:48		
DNI	922.7 W/m^2	Avg. absorber tube outlet temperature	816.2°C
Number of heliostats	38	Absolute humidity	4.34 g/kg
Wind speed [m/s]	5.9 m/s	Receiver pressure in the inlet pipe	3.84 bara
Wind directions	101.9°north	Mass flow	0.526 kg/s
Turbine power	69.96 kW	Pressure drop	73.3 mbar
Turbine speed	97.9	Solar input	291.5 kW
Receiver inlet temperature	594.2°C	Thermal receiver power	125.4 kWth
Receiver outlet temperature	803.2°C	Receiver efficiency	43.0%

Table 2: Results of operation with quartz window

2.4 Comparison to simulations

Simulated efficiencies of 67.7% for the open aperture configuration and 80.8% for the quartz window configuration under full load conditions were presented in [2]. The measured efficiencies of 39.7% and 43% are significantly below these values. Even though in [2] the losses in the collector and the cavity wall were not included, the discrepancy is very high. Two reasons for this were found:

First the heat loss through the cavity walls was much too high. Designed for a loss of 10kW at design conditions with a average wall temperature of 780°C the cavity showed a measured loss of more than 70kW when the aperture was closed with insulation and the turbine was operated only with fuel heating the receiver to an inlet temperature of 550°C. Design flaws of the cavity were a) the use of insulation material without previous heat treatment and b) a weak external mounting structure. As the cavity was heated for the first time after the construction the insulation material started to shrink and as the temperatures at the front side were higher, a stronger shrinkage at the front bent the insulation sheets, thus opening gaps. The weak mounting structure also contributed to these gaps resulting in a strong air exchange of the cavity with the ambient. In addition, the outer walls of the cavity were perforated, allowing uncontrolled air passing through the walls.

Second, the turbine didn't deliver the expected mass flow of about 0.77kg/s minus the small burner mass flows, but only about 75%. An internal leakage in the turbine is suspected as the mass flow equipment didn't show any errors and the receiver pressure drop is smaller than expected.

Both problems could not be solved in the project due to time and budget limitations, but are not seen as obstacles for the technology as they can be solved easily in the future.

2.5. Lessons learned

- Cavity insulation material has to be heat-treated before installation, the mounting structure has to be stiff and must prevent uncontrolled air leakage.
- Wind induced oscillations of the cavity walls affected the cavity insulation. A stiffer mounting structure will also solve this problem.
- Dust from the insulation material was found on the absorber tubes. A dust-tight layer at the inner side of the receiver would prevent this.
- A receiver bypass would allow a faster turbine start-up. The thermal power limit of the combustion chamber is limited to $400kW_{th}$ and as the thermal mass of the receiver cools the combustion chamber inlet temperature down to ambient temperature at the begin of a cold start, the turbine inlet temperature can only be raised as the temperature of the receiver rises. Furthermore, the turbine control has to limit the fuel into the combustion chamber not to exceed the thermal power limit of it.

3. Commercial design

The design of the tested receiver had to follow the boundary conditions of the CESA-1 tower and heliostat field. In a commercial application a more favorable configuration could be chosen. A higher aperture inclination reduces the convection loss without the need of a quartz window, as the buoyancy driven air mass exchange with the ambient reduces, at least at windless conditions. Furthermore, the use of small heliostats is especially beneficial for small tower systems. The low thermal power of the receiver compared to other tower systems results in a small total receiver aperture area and only small heliostats lead to low astigmatism effects. Bigger heliostats result in bigger apertures to limit the spillage loss of the field in off-design points, but at the cost of lower receiver efficiency. A heliostat field configuration with the extreme parameters of a receiver inclination of 90° (horizontal aperture) and a heliostat size of only $1m^2$ is shown in Fig. 3 and Fig. 4.

Fig. 3: Face-down receiver configuration (horizontal aperture)

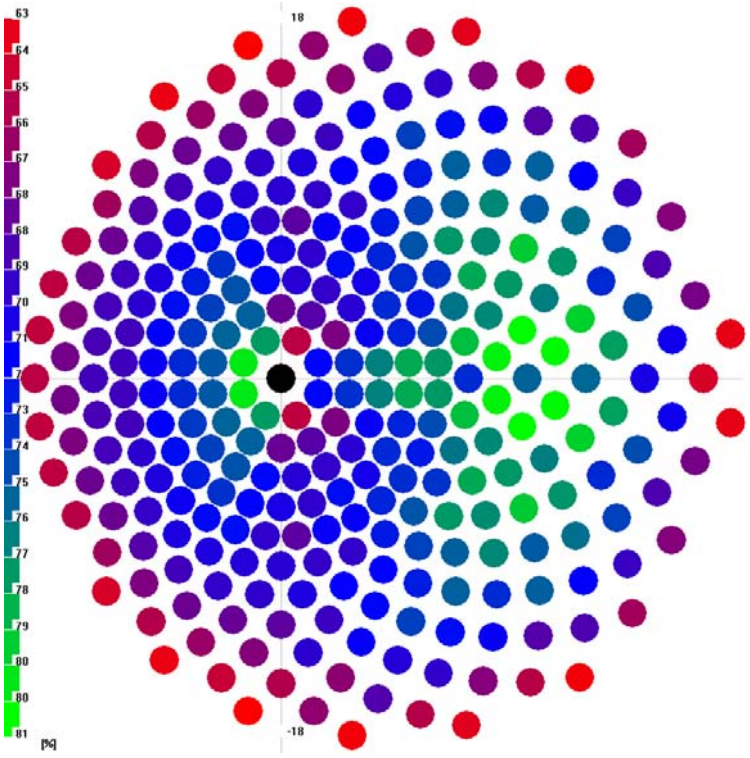

Fig. 4: Commercial heliostat field design for a face-down receiver configuration with single heliostat annual efficiencies (black dot represents tower position)

The heliostats are arranged in a surround field. At 37.2° latitude the heliostat field achieves a favorable annual efficiency of 62.7% with 297 heliostats at a tower height of only 14m and an aperture area of only 0.219m^2, nearly a third of the aperture area of the tested system. In lower latitudes the configuration performs even better. The blocking of radiation by the receiver holding structure is not included in the analysis yet, but is expected to be low with a large enough diameter of the structure. The receiver efficiency for the same tube geometry as in the test was simulated using a 3D-FEM model coupled with a ray-tracer presented in [3]. The model was extended to include the wall losses through a 150mm microporous insulation, also an extreme value and the free convection loss was also included, using the modified Stine & McDonald Nusselt correlation from [4]. Table 3 shows the low combined losses of 12.9%, achieved mainly due to the high

cavity inclination and the small aperture. Forced convection effects due to wind are not included yet, as no Nusselt correlation is available yet, but are expected to have a big effect on the convection loss.

Input	Solar input	212.4 kW	100.0 %
Losses	Reflection	4.0 kW	1.9 %
	Thermal radiation	17.6 kW	8.8 %
	Convection	2.1 kW	1.0 %
	Conduction through the wall	3.7 kW	1.7 %
	Total	27.4 kW	12.9 %
Sum	**Output/efficiency**	**185.1 kW**	**87.1 %**

Table 3: Receiver design point efficiency

4. Solar-hybrid microturbine system with storage

4.1 System description

As shown in [1] solar-hybrid microturbine systems without storage achieve only a solar share of about 25% depending on the load profile. One possibility to deploy a storage system and thus enhance the solar share is shown in Fig. 5.

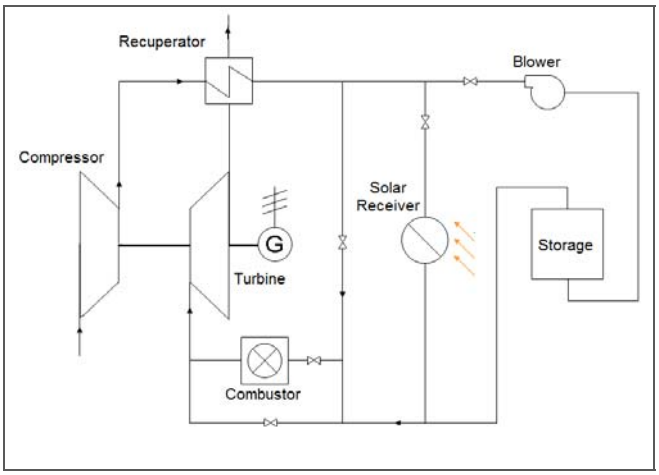

Fig. 5: Scheme of a microturbine system with storage

A storage loop with a pressurized pebble bed storage and a blower are connected in parallel to the receiver. The turbine inlet temperature (TIT) is reduced to 800°C to achieve 100%-solar share at full load of the system. This reduces the maximum power of the turbine from 109kW (at 950°C original TIT) to 75kW and the efficiency to 25.7% from 32%. A bigger receiver and a larger heliostat field provide more energy to the system during the day than can be used directly by the turbine. The excess energy is used to charge the storage by operation of the blower, introducing an air flow through the receiver that is greater than the compressor mass flow. If the solar radiation is not sufficient the blower is not operating and a part or the full air mass flow from the compressor will be directed through the storage where it will be heated to about 800°C (discharge mode). The division of the flow is controlled by valves in front of the receiver and the storage loop which keep the receiver outlet temperature at 800°C or to fully bypass the receiver when the radiation is too low.

An optional combustion chamber provides full dispatchability even when the storage is empty or could also boost the system to the original performance at the cost of fuel consumption. Two optional bypasses at the receiver and at the combustion chamber reduce pressure losses in the system.

4.2 Results

The following table shows selected results for the solar gas turbine system with storage for an off-grid load [5].

Receiver capacity	794 kW_{th}	Particle diameter	3.2 mm
Solar multiple	2.7	Storage pressure drop	24 mbar
Annual field efficiecy	66%	Blower power	11 kW
Storage capacity	9 h	Blower annual electric consumption	10 MWh_{el}
Storage height	3.8 m	Annual electricity production (net)	343 MWh_{el}
Storage diameter	3.7 m	Solar share	82%

Table 4: System parameters and results

4.3. Discussion

The system parameters in Table 4 show a storage configuration with enough capacity to allow a solar share of 82% while the pressure drop over the storage is only 24mbar. Therefore the blower power is mainly affected by the receiver pressure drop. The blower power of 11 kW is quite high compared to the turbine output of 75kW, but as the blower operates in part load or is shut off most of the time the annual electric consumption of the blower is only 10 MWh.

5. Conclusions and Outlook

The tube receiver and the system were successfully tested in more than 100h solar operation with the design outlet temperature of 800°C reached in both open aperture and pressureless quartz window configuration without any receiver failure. The very low efficiencies measured are not representative for the technology but due to first prototype problems. The perspective to combine the receiver technology with pressurized pebble bed heat storage opens up the off-grid market to the promise of power around the clock with high solar shares.

The follow-up demonstration project SMILE, co-funded by the German Ministry of the Environment in the International Climate Initiative is currently under way.

6. Acknowledgements

This work was co-funded by the European Commission as part of the SOLHYCO-project (Contract No. 19830).

References

[1] L. Amsbeck, R. Buck, P. Heller, J. Jedamski, R. Uhlig: Development of a Tube Receiver for a Solar-Hybrid Microturbine System, Solarpaces 2008, March 4-7, Las Vegas, USA

[2] Uhlig R., Amsbeck L., Helsch G., Röger M. , Development of a Broadband Antireflection Coated Transparent Silica Window for a Solar-Hybrid Microturbine System, Solarpaces 2009, Berlin, Germany

[3] S. Ulmer: Messung der Strahlungsflussdichte-Verteilung von punktkonzentrierenden solarthermischen Kraftwerken, Phd thesis (in German), University of Stuttgart (2003)

[4] S. Paitoonsurikarn: Study of a Dissociation Reactor for an Ammonia-Based Solar Thermal System, Phd-thesis, Australian National University (2006)

[5] T. Prosinečki, Design and performance analysis of a small scale Brayton cycle concentrated solar power tower with regenerative thermal storage, Master thesis, Royal Institute of Technology and the German Aerospace Center (2010)